2 Experimental measurements of intracellular mechanics

Paul Janmey and Christoph Schmidt

ABSTRACT: Novel methods to measure the viscoelasticity of soft materials and new theories relating these measurements to the underlying molecular structures have the potential to revolutionize our understanding of complex viscoelastic materials like cytoplasm. Much of the progress in this field has been in methods to apply piconewton forces and to detect motions over distances of nanometers, thus performing mechanical manipulations on the scale of single macromolecules and measuring the viscoelastic properties of volumes as small as fractions of a cell. Exogenous forces ranging from pN to nN are applied by optical traps, magnetic beads, glass needles, and atomic force microscope cantilevers, while deformations on a scale of nanometers to microns are measured by deflection of lasers onto optical detectors or by high resolution light microscopy.

Complementary to the use of external forces to probe material properties of the cell are analyses of the thermal motion of refractile particles such as internal vesicles or submicron-sized beads imbedded within the cell. Measurements of local viscoelastic parameters are essential for mapping the properties of small but heterogeneous materials like cytoplasm; some methods, most notably atomic force microscopy and optical tracking methods, enable high-resolution mapping of the cell's viscoelasticity.

A significant challenge in this field is to relate experimental and theoretical results derived from systems on a molecular scale to similar measurements on a macroscopic scale, for example from tissues, cell extracts, or purified polymer systems, and thus provide a self-consistent set of experimental methods that span many decades in time and length scales. At present, the new methods of nanoscale rheology often yield results that differ from bulk measurements by an order of magnitude. Such discrepancies are not a trivial result of experimental inaccuracy, but result from physical effects that only currently are being recognized and solved. This chapter will summarize some recent advances in methodology and provide examples where experimental results may motivate new theoretical insights into both cell biology and material science.

Introduction

The mechanical properties of cells have been matters of study and debate for centuries. Because cells perform a variety of mechanical processes, such as locomotion, secretion, and cell division, mechanical properties are relevant for biological function. Certain cells, such as plant cells and bacteria, have a hard cell wall that dominates

the mechanics, whereas most other cells have a soft membrane and their mechanical properties are determined largely by an internal protein polymer network, the cytoskeleton. Early observations of single cells by microscopy showed regions of cytoplasm that were devoid of particles undergoing Brownian motion, and therefore were presumed to be "glassy" (see Chapter 3) or in some sense solid (Stossel, 1990). The interior of the cell, variously called the protoplasm, the ectoplasm, or more generally the cytoplasm, was shown to have both viscous and elastic features. A variety of methods were designed to measure these properties quantitatively.

Forces to which cells are exposed in a biological context

The range of stresses (force per area) to which different tissues are naturally exposed is large. Cytoskeletal structures have evolved accordingly and are not only responsible for passively providing material strength. They are also intimately involved in the sensing of external forces and the cellular responses to those forces. How cells respond to mechanical stress depends not only on specific molecular sensors and signaling pathways but also on their internal mechanical properties or rheologic parameters, because these material properties determine how the cell deforms when subjected to force (Janmey and Weitz, 2004).

It is likely that different structures and mechanisms are responsible for different forms of mechanical sensing. For example, cartilage typically experiences stresses on the order of 20 MPa, and the individual chondrocytes within it alter their expression of glycosaminoglycans and other constituents as they deform in response to such large forces (Grodzinsky et al., 2000). Bone and the osteocytes within it respond to similarly large stresses (Ehrlich and Lanyon, 2002), although the stress to which a cell imbedded within the bone matrix is directly exposed is not always clear. At the other extreme, endothelial cells undergo a wide range of morphological and transcriptional changes in response to shear stresses less than 1 Pa (Dewey et al., 1981), and neutrophils activate in response to similar or even smaller shear stresses (Fukuda and Schmid-Schonbein, 2003). Not only the magnitude but the geometry and time course of mechanical perturbations are critical to elicit specific cellular effects. Some tissues like tendons or skeletal muscle experience or generate mainly uniaxial forces and deformations, while others, such as the cells lining blood vessels, normally experience shear stresses due to fluid flow. These cells often respond to changes in stress or to oscillatory stress patterns rather than to a specific magnitude of stress (Bacabac et al., 2004; Davies et al., 1986; Florian et al., 2003; Ohura et al., 2003; Turner et al., 1995). Many cells, including the cells lining blood vessels and epithelial cells in the lung, experience large-area-dilation forces, and in these settings both the magnitude and the temporal characteristics of the force are critical to cell response (Waters et al., 2002).

Methods to measure intracellular rheology by macrorheology, diffusion, and sedimentation

The experimental designs to measure cytoplasmic (micro)rheology have to overcome three major challenges: the small size of the cell; the heterogeneous structure of the cell interior; and the active remodeling of the cytoplasm that occurs both constitutively,

as part of the resting metabolic state, and directly, in response to the application of forces necessary to perform the rheologic measurement. The more strongly the cell is perturbed in an effort to measure its mechanical state, the more it reacts biochemically to change that state (Glogauer et al., 1997). Furthermore it is important to distinguish linear response to small strains from nonlinear response to larger strains. Structural cellular materials typically have a very small range of linear response (on the order of 10 percent) and beyond that react nonlinearly, for example by strain hardening or shear thinning or both in sequence. To overcome these problems a number of experimental methods have been devised.

Whole cell aggregates

The simplest and in some sense crudest method to measure intracellular mechanics is to use standard rheologic instruments to obtain stress/strain relations on a macroscopic sample containing many cells, but in which a single cell type is arranged in a regular pattern. Perhaps the most successful application of this method has been the study of muscle fibers, in which actin-myosin-based fibers are arranged in parallel and attached longitudinally, allowing an inference of single cell quantities directly from the properties of the macroscopic sample. One example of the validity of the assumptions that go into such measurements is the excellent agreement of single molecule measurements of the force-elongation relation for titin molecules with macroscopic compliance measurements of muscle fibers where the restoring force derives mainly from a large number of such molecules working in series and in parallel (Kellermayer et al., 1997). Another simple application of this method is the measurement of close-packed sedimented samples of a single cell type, with the assumption that during measurement, the deformation is related to the deformation of the cell interior rather than to the sliding of cells past each other. Such measurement have, for example, shown the effects of single actin-binding protein mutations in Dictyostelium (Eichinger et al., 1996) and melanoma cells (Cunningham et al., 1992). These simple measurements have the serious disadvantage that properties of a single cell require assumptions or verification of how the cells attach to each other, and in most cases the contributions of membrane deformation cannot be separated from those of the cell interior or the extracellular matrix.

Sedimentation of particles

To overcome the problems inherent in the measurement of macroscopic samples, a variety of elegant solutions have been devised. Generally, in order to resolve varying viscoelastic properties within a system, one has to use probes of a size comparable to or smaller than the inhomogeneities. Such microscopic probes can be fashioned in different ways. One of the simplest and oldest methods to measure cytoplasmic viscosity relies on observations of diffusion or sedimentation of intracellular granules with higher specific gravity through the cytoplasmic continuum. Generally these measurements were performed on relatively large cells containing colored or retractile particles easily visible in the microscope. Such measurements (reviewed in Heilbrunn, 1952; Heilbrunn, 1956) are among the earliest to obtain values similar to

those measured currently, but they are limited to specialized cells and cannot measure elasticity in addition to viscosity.

Sedimentation measurements are done by a variety of elegant methods. One of the earliest such studies (Heilbronn, 1914) observed the rate of falling of starch grains within a bean cell and compared the rate of sedimentation of the same starch particles purified from the cells in fluids of known densities and viscosities measured by conventional viscometers, to obtain a value of 8 mPa.s for cytoplasmic viscosity. These measurements were an early application of a falling-sphere method commonly used in macroscopic rheometry (Rockwell et al., 1984). The viscosity of the cytoplasm in this application was determined by relation to calibrated liquids; because the starch particles are relatively uniform and could be purified from the cell, inaccuracies associated with measurement of their small size were avoided. More generally, any gravity-dependent velocity V of a particle of radius r and density σ in the cytoplasm of density ρ could be used to measure cytoplasmic viscosity η by use of the relation

$$V = \frac{2g(\sigma - \rho)r^2}{9\eta}, \tag{2.1}$$

in which g is the gravitational acceleration. Without centrifugation internal organelles rarely sediment, but a sufficiently large density difference between an internal particle and the surrounding cytoplasm could be created by injecting a small droplet of inert oil into a large cell, like a muscle fiber (Reiser, 1949) to obtain values of 29 mPa.s from the rate at which the drop rose in the cytoplasm. Alternatively, internal organelles could be made to sediment by known gravitational forces in a centrifuge, and in various cells – including oocytes, amoebas, and slime molds – cytoplasmic viscosities between 2 and 20 mPa.s have been commonly reported, although some much higher values greater than 1 Pa.s were also observed (reviewed in Heilbrunn, 1956). The large differences in viscosity were presumed to arise from experimental differences in the sedimentation rates, because these early studies also showed that cytoplasm was a highly non-Newtonian fluid and that the apparent viscosity strongly decreased with increasing shear rate.

Diffusion

Measurements of viscosity by diffusion (Heilbrunn, 1956) have been done by first centrifuging a large cell, such as a sea urchin egg or an amoeba, with sedimentation forces typically between 100 and 5000 times that of gravity, sufficient for internal organelles to get concentrated at the bottom while the cell remains intact. Then the displacement of a single particle of radius r in one direction $x(t)$ is monitored, and the cytoplasmic viscosity is measured from the Stokes-Einstein relation:

$$\langle x^2(t) \rangle = \frac{k_B T}{3\pi\eta r}, \tag{2.2}$$

where the brackets denote ensemble averaging, k_B is the Boltzmann constant, and T is temperature. Such measurements, dating from at least the 1920s (decades before video microscopy and image processing) showed that the viscosity within sea urchin egg cytoplasm was 4 mPa.s (4 cP), only four times higher than that of water, but that other

cells exhibited much higher internal viscosities. Three other important features of intracellular material properties were evident from these studies. First, it was shown that the apparent viscosity of the protoplasm depended strongly on flow rates, as varied, for example, by changing the sedimentation force in the centrifuge. Second, viscous flow of internal organelles could generally be measured only deeper inside the cell, away from the periphery, where an elastic cortical layer could be distinguished from the more liquid cell interior. Third, the cellular viscosity was often strongly temperature dependent.

Mechanical indentation of the cell surface

Glass microneedles

Glass needles can be made thin enough to apply to a cell measured forces large enough to deform it but small enough that the cell is not damaged. An early use of such needles was to pull on individual cultured neurons (Bray, 1984); these studies showed how such point forces could be used to initiate neurite extension. Improved instrumentation and methods allowed an accurate estimate of the forces needed to initiate these changes. The method (Heidemann and Buxbaum, 1994; Heidemann et al., 1999) begins with calibration of the bending constant of a wire needle essentially by hanging a weight from the end of a thin metal wire and determining its spring constant from deflection of the loaded end by the relation:

$$y(L) = \frac{FL^3}{3EI} \tag{2.3}$$

where $y(L)$ is the displacement of the end of a wire of length L, F is the force due to the weight, E is the material's Young's modulus of elasticity, and $I = \pi r^4/4$ is the second moment of inertia of the rod of radius r.

The product EI is a constant for each rod; in practice the first calibrated rod is used to provide a known (smaller) force to a thinner, usually glass, rod, to calibrate that rod, and repeat the process until a rod is calibrated that can provide nN or smaller forces depending on its length and radius.

Cell poker

A pioneering effort to apply forces locally to the surface of live cells was the development of the cell poker (Daily et al., 1984; Petersen et al., 1982). In this device, shown schematically in Fig. 2-1, a cell is suspended in fluid from a glass coverslip on an upright microscope, below which is a vertical glass needle attached at its opposite end to a wire needle that is in turn coupled to a piezoelectric actuator that moves the wire/needle assembly up and down. The vertical displacements of both ends of the wire are measured optically, and a difference in the displacements of these points, x, occurs because of resistance to moving the glass needle tip as it makes contact with the cell. The force exerted by the tip F on the cell surface is determined by Hooke's law $F = kx$ from the stiffness of the wire k, which can be calibrated by macroscopic means such as the hanging of known weights from a specified length of wire. Using this

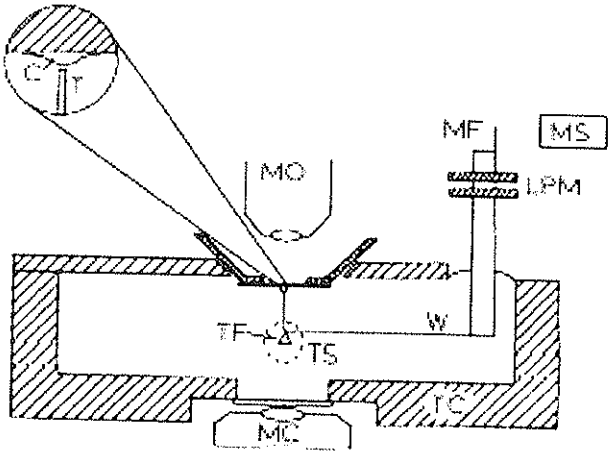

Fig. 2-1. Schematic representation of the cell-poking apparatus. Positioning of the cell (C) relative to the poker tip (T) is achieved by translating the top of the temperature control unit (TC) or by rotating the holder on which the coverslip is mounted. The motor assembly can be translated to ensure the tip is positioned in the field of view. W, steel wire; LPM, linear piezoelectric motor; MS and TS, optical sensors; MF, motor flag; TF, tip flag; MO, modulation contrast objective; MC, matching condenser.

instrument, displacements less than 100 nm can be resolved corresponding to forces less than 10 nN. A typical force vs. displacement curve from this instrument as shown in Fig. 2-2 reveals a significant degree of both elasticity and unrecoverable deformation from plasticity or flow of the cytoplasm. Such measurements have demonstrated both a significant elastic response as well as a plastic deformation of the cell, and the time course and magnitudes of these processes can be probed by varying the rate at which the forces are applied. Because the tip is considerably smaller than the cross-sectional area of the cell, local viscoelasticity could be probed at different regions of the cell or as active motion or other responses are triggered. The earliest such measurements revealed a large difference in relative stiffness over different areas of the cell and a high degree of softening when actin-filament-disorganizing drugs like

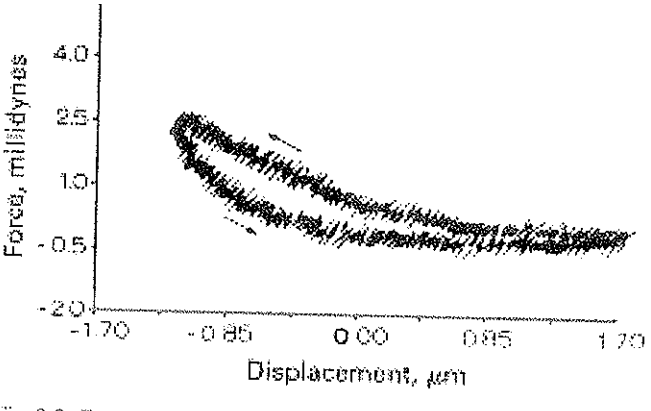

Fig. 2-2. Force displacement curve as the cell poker tip first indents the cell (upper curve) and then is lowered away from the cell contact (lower curve).

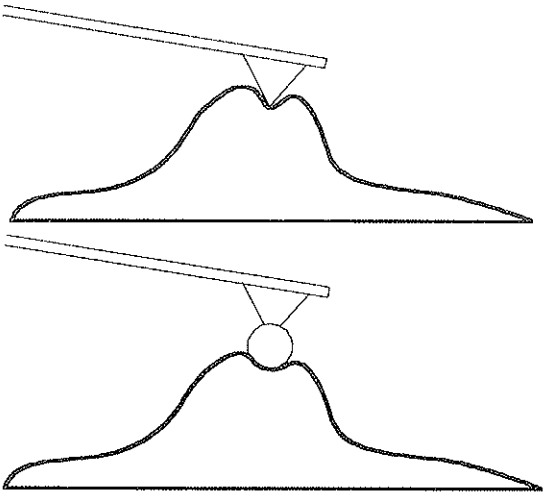

Fig. 2-3. Cell poking with the tip of an atomic force microscope. Upper image: If a regular sharp tip is used, inhomogeneities encountered on the nm scale of the tip radius are likely to make the result difficult to interpret. Lower image: Using a micrometer-sized bead attached to the tip, force sensitivity is maintained while the cell response is averaged over a micrometer scale.

cytochalasin were applied. The measurements also showed that the apparent stiffness of the cell increased as the amplitude of indentation increased. How this nonlinear elastic response is related to the material properties of the cell is, however, not straightforward to deduce, because of a number of complicating effects, as the earliest such studies pointed out.

For a homogeneous, semi-infinite elastic solid, given the geometry of the glass needle tip and the force of indentation, the force-displacement curves are determined by two material properties, the Young's modulus and Poisson's ratio, in a way that is described by the Hertz relation. For a sphere the result for the force as a function of indentation depth δ is (Hertz, 1882; Landau and Lifshitz, 1970):

$$F_{sphere} = \frac{4}{3}\frac{E}{(1-\nu^2)} R^{1/2}\delta^{3/2} \tag{2.4}$$

with the Young's modulus E, Poisson ratio ν, and sphere radius R. For indentation with a conical object, the result is:

$$F_{cone} = \frac{\pi}{2}\frac{E}{(1-\nu^2)} \tan(\alpha)\,\delta^2 \tag{2.5}$$

with the cone opening angle α.

The application of the Hertz model in relation to cell-poking measurements is, however, often not meaningful for at least three reasons. First, the Hertz relation is not valid if the cell thickness is not much greater than the degree of indentation. Second, the cell cytoskeleton is in most cases far from being an isotropic homogeneous material. And third, forces exerted on a cell typically initiate biochemical as well as other active reactions. These issues have been extensively discussed both in terms of the cell poker (Daily et al., 1984), and more recently in applications of the scanning force microscope that operates on the same principle.

Atomic force microscopy

A very sensitive local mechanical probe is provided by atomic force microscopy (AFM). An AFM in an imaging mode works by scanning a sharp microfabricated tip over a surface while simultaneously recording tip deflection. The deflection time course is then converted into an image of the surface profile (Binnig et al., 1986). Imaging can be done in different modes – contact mode (Dufrene, 2003), tapping mode (Hansma et al., 1994), jumping mode (de Pablo et al., 1998) or others – which are usually designed to minimize damage to the sample or distortions of the surface by the imaging method. When one wants to probe the mechanical properties of a material surface, however, one can also use an AFM tip to exert precisely controlled forces in selected locations and record the corresponding sample displacements. In many ways this method is related to cell poking with larger probes, but it holds the potential of better spatial and force resolution. The obvious limitation of the technique is that manipulation can only occur through the accessible surface of a cell, that is one cannot measure elastic moduli well inside the cell without an influence of boundary conditions. One can both indent cells or pull on cells when the tips are attached strongly enough to the cell surface. The indentation approach has been used to test the elastic properties of various types of cell. Initial studies have used conventional sharp (radius of 10s of nm) tips and applied the Hertz model as described above (reviewed in MacKintosh and Schmidt, 1999). The same caveats hold in this case as in the discussion of other cell-poking experiments: the cell is not a homogeneous, isotropic, passive elastic solid. The thin parts of cells, at the cell periphery in surface-attached cells, are particularly interesting to study because they are crucial for cell motility but are usually too thin to apply the standard Hertz model. When using an AFM with a sharp tip, the spatial inhomogeneity of cells – for example the presence of bundles of actin (stress fibres), microtubules, and more – is likely more of a problem, because spatial averaging in the case of a larger probe tends to make the material look more homogeneous. Results of initial experiments were thus rather qualitative, but differences between the cell center and its periphery could be detected (Dvorak and Nagao, 1998). A problem with quasi-static or low-frequency measurements is that the cell will react to forces exerted on it and the response measured will not only reflect passive material properties, but also active cellular responses. AFM has also been used on cells in a high-frequency mode, namely the tapping mode. It was observed that cells dynamically stiffened when they were probed with a rapidly oscillating tip, as one would expect (Putman et al., 1994).

A more quantitative technique has been developed more recently, using polystyrene beads of carefully controlled radius attached to the AFM tips to contact cells (Mahaffy et al., 2004; Mahaffy et al., 2000). This creates a well-defined probe geometry and provides another parameter, namely bead radius, to control for inhomogeneities. Values for zero-frequency shear moduli were between 1 and 2 kPa for the fibroblast cells studied. The probing was in this case also done with an oscillating tip, to measure frequency-dependent viscoelastic response with a bandwidth of 50–300 Hz and data were evaluated with an extended Hertz model valid for oscillating probes (Mahaffy et al., 2000). A problem for determining the viscous part of the response is the hydrodynamic drag on the rest of the cantilever that dominates and changes

with decreasing distance from the surface and with tip-sample contact and is not easy to correct for.

The Hertz model has been further modified to account for finite sample thickness and boundary conditions on the substrate (Mahaffy et al., 2004), which makes it possible to estimate elastic constants also for the thin lamellipodia of cells, which were found again to be between 1 and 2 kPa in fibroblasts.

Mechanical tension applied to the cell membrane

Pulling on a cell membrane by controlled suction within a micropipette has been an important tool to measure the viscosity and elastic response of cells to controlled forces. The initial report of a cell elastimeter based on micropipette aspiration (Mitchison and Swann, 1954) has guided many studies that have employed this method to deform the membranes of a variety of cells, especially red blood cells, which lack a three-dimensional cytoskeleton but have a continuous viscoelastic protein network lining their outer membrane (Discher et al., 1994; Evans and Hochmuth, 1976). One important advantage of this method is that the cell can either be suspended in solution while bound to the micropipette or attached to a surface as the micropipette applies negative pressure from the top. The ability to probe nonadherent cells has made micropipette aspiration a powerful method to probe the viscoelasticity of blood cells including erythrocytes, leukocytes, and monocytes (Chien et al., 1984; Dong et al., 1988; Richelme et al., 2000).

A typical micropipette aspiration system is shown in Fig. 2-4. Images of two red blood cells partly pulled into a micropipette are shown in Fig. 2-5. Micropipette aspiration provides measures of three quantities: the cortical tension in the cell membrane; the cytoplasmic viscosity; and the cell elasticity. If the cell can be modeled as a liquid drop with a cortical tension, as appears suitable to leukocytes under some conditions, the cortical tension t is calculated from the pressure at which the aspirated part of the cell forms a hemispherical cap within the pipette.

For a cell modeled as an elastic body, its Young's modulus E is determined by the relation

$$\Delta P = \frac{2\pi}{3} E \frac{L_p}{R_p} \phi, \tag{2.6}$$

where ΔP is the pressure difference inside and outside the pipette, L_p is the length of the cell pulled into the pipette with radius R_p, and ϕ is a geometric constant with a value around 2.1 (Evans and Yeung, 1989).

For liquid-like flow of cells at pressures exceeding the cortical tension, the cytoplasmic viscosity is calculated from the relation

$$\eta = \frac{R_p \Delta p}{\left(\frac{dL_p}{dt}\right) m(1 - R_p/R)}, \tag{2.7}$$

where η is the viscosity, R is the diameter of the cell outside the pipette, and m is a constant with a value around 9 (Evans and Yeung, 1989).

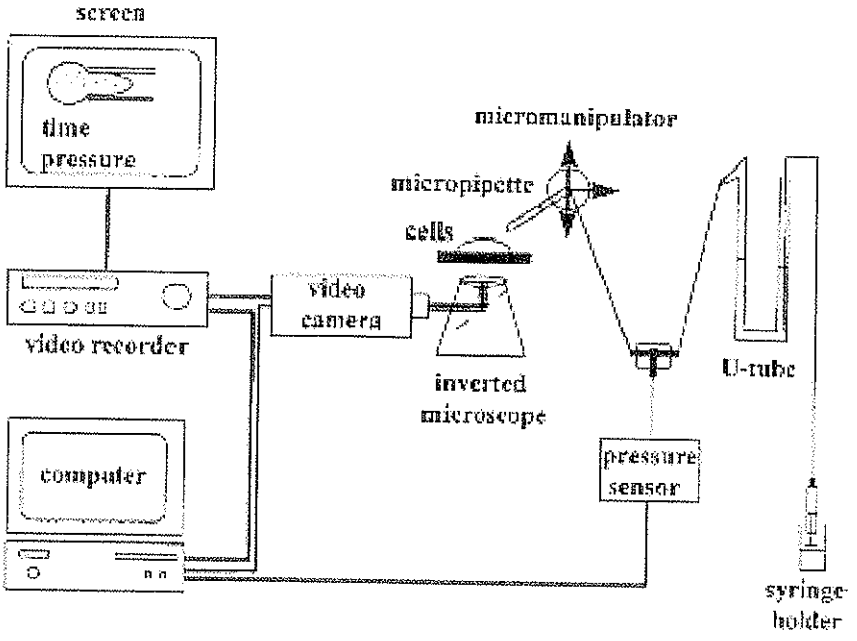

Fig. 2-4. Experimental study of cell response to mechanical forces. Cells are deposited on the stage of an inverted microscope equipped with a video camera. The video output is connected to a digitizer mounted on a desk computer. Cells are aspirated into micropipettes connected to a syringe mounted on a syringe holder. Pressure is monitored with a sensor connected to the computer. Pressure and time values are superimposed on live cell images before recording on videotapes for delayed analysis. From Richelme et al., 2000.

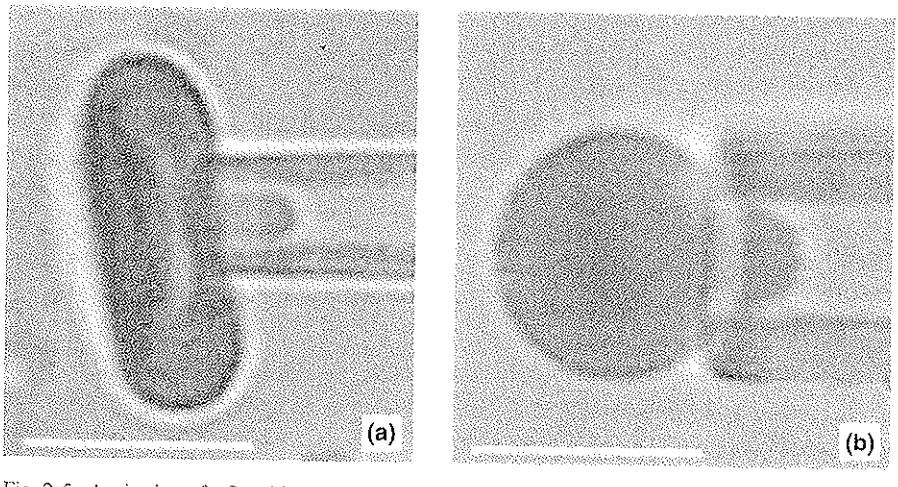

Fig. 2-5. Aspiration of a flaccid (a) and swollen (b) red blood cell into a pipette. The diameter of the flaccid cell is approximately 8 μm and that of the swollen cell is about 6 μm. The scale bars indicate 5 μm. From Hochmuth, 2000.

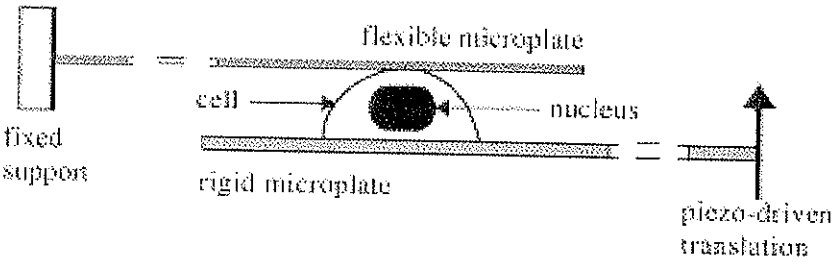

Fig. 2-6. Diagram for a device for compression of a cell between microplates. Variations of this design also allow for imposition of shear deformation. From Caille et al., 2002.

Shearing and compression between microplates

For cells that normally adhere to surfaces, an elegant but technically challenging method to measure viscoelasticity is by attaching them at both top and bottom to glass surfaces that can be moved with respect to each other in compression, extension, or shear (Thoumine et al., 1999). A schematic diagram of such a system is shown in Fig. 2-6.

In this method a cell such as a fibroblast that adheres tightly to glass surfaces coated with adhesion proteins such as fibronectin is grown on a relatively rigid plate; a second, flexible plate is then placed on the top surface. Piezo-driven motors displace the rigid plate a known distance to determine the strain, and the deflection of the flexible microplate provides a measure of the stress imposed on the cell surface. Use of this device to provide well-defined strains with simultaneous imaging of internal structures such as the nucleus provides a measure of the elastic modulus of fibroblasts around 1000 Pa, consistent with measurements by AFM, and has shown that the stiffness of the nucleus is approximately ten times greater than that of the cytoplasmic protein networks (Caille et al., 2002; Thoumine and Ott, 1997). A recent refinement of the microcantilever apparatus allows a cell in suspension to be captured by both upper and lower plates nearly simultaneously and to measure the forces exerted by the cell as it begins to spread on the glass surfaces (Desprat et al., 2005).

Fluid flow

Cells have to withstand direct mechanical deformations through contact with other cells or the environment, but some cells are also regularly exposed to fluid stresses, such as vascular endothelial cells in the circulating system or certain bone cells (osteocytes) within the bone matrix. Cells sense these stresses and their responses are crucial for many regulatory processes. For example, in vascular endothelial cells, mechanosensing is believed to control the production of protective extracellular matrix (Barbee et al., 1995; Weinbaum et al., 2003); whereas in bone, mechanosensing is at the basis of bone repair and adaptive restructuring processes (Burger and Klein-Nulend, 1999; Wolff, 1986). Osteocytes have been studied *in vitro* after extraction from the bone matrix in parallel plate flow chambers (Fig. 2-7). Monolayers of osteocytes coated onto one of the chamber surfaces were exposed to shear stress while the

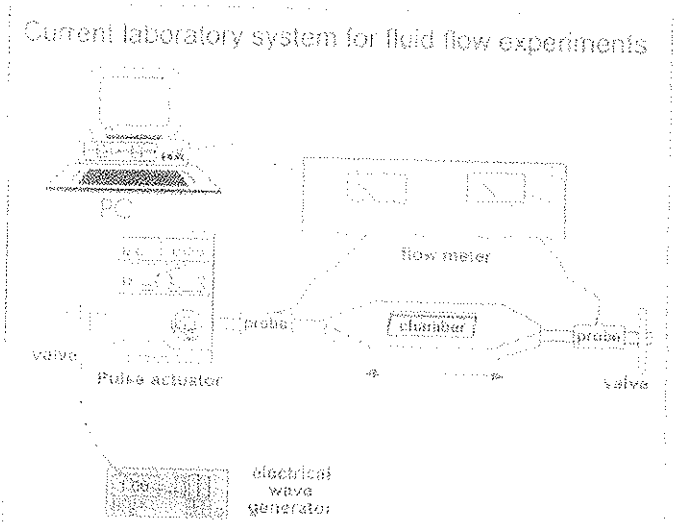

Fig. 2-7. Fluid flow system to stimulate mechanosensitive bone cells, consisting of a culture chamber containing the cells, a pulse generator controlling the fluid flow, and flow meters. The response of the cells is either biochemically measured from the cells after the application of flow (for example prostaglandin release) or measured in the medium after flowing over the cells (for example nitric oxide). From Klein-Nulend et al., 2003.

response was measured by detecting the amount of nitric oxide produced as a function of fluid flow rate (Bacabac et al., 2002; Rubin and Lanyon, 1984).

The strain field within individual surface-attached cells in response to shear flow has been mapped in bovine vascular endothelial cells with the help of endogenous fluorescent vimentin (Helmke et al., 2003; Helmke et al., 2001). It was found that the spatial distribution of strain is rather inhomogeneous, and that strain is focused to localized areas within the cells. The method can only measure strain and not stress. The sites for mechanosensing might be those where strain is large if some large distortion of the sensing element is required to create a signal, in other words, if the sensor is "soft." On the other hand, the sites for sensing might also be those where stress is focused and where little strain occurs if the sensing element requires a small distortion, or is "hard," and functions by having a relatively high force threshold.

Numerical simulations can be applied to both the cell and the fluid passing over it. A combination of finite element analysis and computational fluid dynamics has been used to model the flow across the surface of an adhering cell and to calculate the shear stresses in different spots on the cell (Barbee et al., 1995; Charras and Horton, 2002). This analysis provides a distribution of stress given a real (to some resolution) cell shape, but without knowing the material inhomogeneities inside, the material had to be assumed to be linear elastic and isotropic. The method was also applied to model stress and strain distributions inside cells that were manipulated by AFM, magnetic bead pulling or twisting, and substrate stretching, and proved useful to compare the effects of the various ways of mechanical distortion.

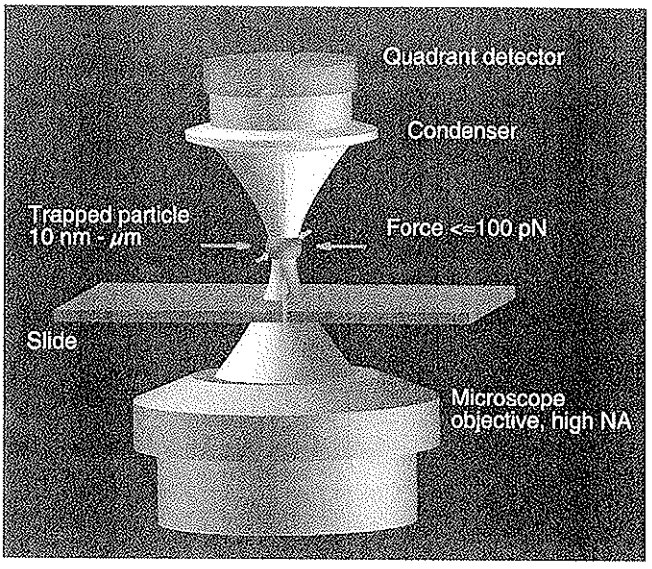

Fig. 2-8. Schematic diagram of an optical trap.

Optical traps

Optical traps (see Fig. 2-8) use a laser beam focused through a high-numerical aperture microscope objective lens to three-dimensionally trap micron-sized refractile particles, usually silica or latex beads (Ashkin, 1997; Svoboda and Block, 1994). The force acting on the bead at a certain distance from the laser focus is in general very difficult to calculate because (1) a high-NA laser focus is not well approximated by a Gaussian, and (2) a micron-sized refractive particle will substantially affect the light field. Approximations are possible for both small particles (Rayleigh limit) and large particles (ray optics limit) with respect to the laser wave length. For a small particle, the force can be subdivided into a "gradient force" pulling the particle towards the laser focus and a scattering force pushing it along the propagation direction of the laser (Ashkin, 1992). Assuming a Gaussian focus and a particle much smaller than the laser wavelength, the gradient forces in radial and axial direction are (Agayan et al., 2002):

$$F_g^{axial} \propto -\alpha' I_0 z \frac{w_0^4}{z_0^2}\left[\frac{1}{w^4(z)} - \frac{2r^2}{w^6(z)}\right] \cdot \exp\left(-\frac{2r^2}{w^2(z)}\right) \tag{2.8}$$

$$F_g^{radial} \propto -\alpha' I_0 r \frac{w_0^2}{w^4(z)} \cdot \exp\left(-\frac{2r^2}{w^2(z)}\right) \tag{2.9}$$

and the scattering forces:

$$F_s^{axial} \propto \alpha'' I_0 \frac{w_0^2}{w^2(z)}\left[k_m\left(1 - \frac{r^2}{2}\frac{\left(z^2 - z_0^2\right)}{\left(z^2 + z_0^2\right)^2}\right) - \frac{w_0^2}{z_0 w^2(z)}\right] \cdot \exp\left(-\frac{2r^2}{w^2(z)}\right) \tag{2.10}$$

$$F_s^{radial} \propto \alpha'' I_0 \frac{w_0^2}{w^2(z)} \frac{k_m r}{R(z)} \exp\left(-\frac{2r^2}{w^2(z)}\right) \tag{2.11}$$

with complex polarizability $\alpha = \alpha' + i\alpha''$, laser intensity I_0, w_0 the beam radius in the focus, and $w(z) = w_0\sqrt{1 + (z/z_0)^2}$ the beam radius near the focus; $z_0 = \pi w_0^2/\lambda_m$ the Rayleigh range, $k_m = 2\pi/\lambda_m$ the wave vector, with λ_m the wavelength in the medium with refractive index n_m. (For details and prefactors see Agayan et al., 2002).

Stable trapping will only occur if the gradient force wins over the trapping force all around the focus. Trap stability thus depends on the geometry of the applied field and on properties of the trapped particle and the surrounding medium. The forces generally depend on particle size and the relative index of refraction $n = n_p/n_m$, where n_p and n_m are the indices of the particle and the medium, respectively, which is hidden in the polarizability α in Eqs. 2.8–2.11. In the geometrical optics regime, maximal trap strength is particle-size-independent, but increases with n over some intermediate range until, at larger values of n, the scattering force exceeds the gradient force. The scattering force on a nonabsorbing Rayleigh particle of diameter d is proportional to its scattering cross-section, thus the scattering force scales with the square of the polarizability (volume) (Jackson, 1975), or as d^6. The gradient force scales linearly with polarizability (volume), that is, it has a d^3-dependence (Ashkin et al., 1986; Harada and Asakura, 1996).

A trappable bead can then be attached to the surface of a cell and can be used to deform the cell membrane locally. The method has the advantage that no mechanical access to the cells is necessary. Using beads of micron size furthermore makes it possible to choose the site to be probed on the cell with relatively high resolution. A disadvantage is that the forces that can be exerted are difficult to increase beyond about 100 pN, orders of magnitude smaller than can be achieved with micropipettes or AFM tips. At high laser powers, local heating may not be negligible (Peterman et al., 2003a). Force and displacement can be detected, however, with great accuracy, sub-nm for the displacement and sub-pN for the force, using interferometric methods (Gittes and Schmidt, 1998; Pralle et al., 1999). This makes the method well suited to study linear response parameters of cells. Interferometric detection can also be as fast as 10 μs, opening up another dimension in the study of cell viscoelasticity. Focusing on different frequency regimes should make it, for example, possible to differentiate between active, motor-driven responses and passive viscoelasticity. Such an application of optical tweezers is closely related to laser-based microrheology, which can also be applied inside the cells (see **Passive Microrheology**). We will here focus on experiments that have used the optical manipulation of externally attached beads.

Optical tweezers have been used by several groups to manipulate human red blood cells (see Fig. 2-9), which have no space-filling cytoskeleton but only a membrane-associated 2D protein polymer network (spectrin network). The 2D shear modulus measured for the cell membrane plus spectrin network varies between 2.5 μN/m (Henon et al., 1999; Lenormand et al., 2001) and 200 μN/m (Sleep et al., 1999), possibly due to different modeling approaches in estimating the modulus. The nonlinear part of the response of red blood cells has been explored by using large beads and high laser power achieving a force of up to 600 pN. The shear modulus of the cells levels off at intermediate forces before rising again at the highest forces, which was simulated in finite element models of the cells under tension (Dao et al., 2003; Lim et al., 2004).

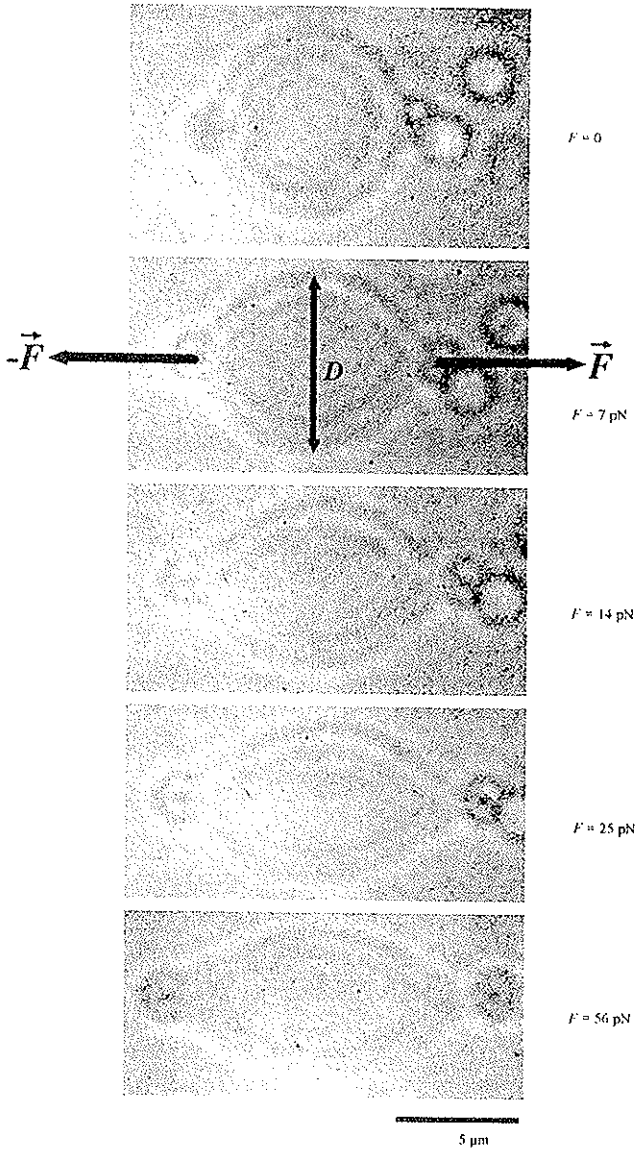

Fig. 2-9. Stretching of red blood cells by optical tweezers, using a pair of beads attached to diametrically opposed ends of the cell. Forces are given next to the panels. From Henon et al., 1999.

Magnetic methods

Using magnetic particles has the advantage that large forces (comparable to AFM) can be exerted, while no open surface is required. One can use magnetic fields to apply forces and/or torques to the particles. Ferromagnetic particles are needed to apply torques; paramagnetic particles are sufficient to apply force only. A disadvantage of the magnetic force method is that it is difficult to establish homogeneous field gradients (only gradients exert a force on a magnetic dipole), and the dipole moments of microscopic particles typically scatter strongly. Furthermore, one is often limited

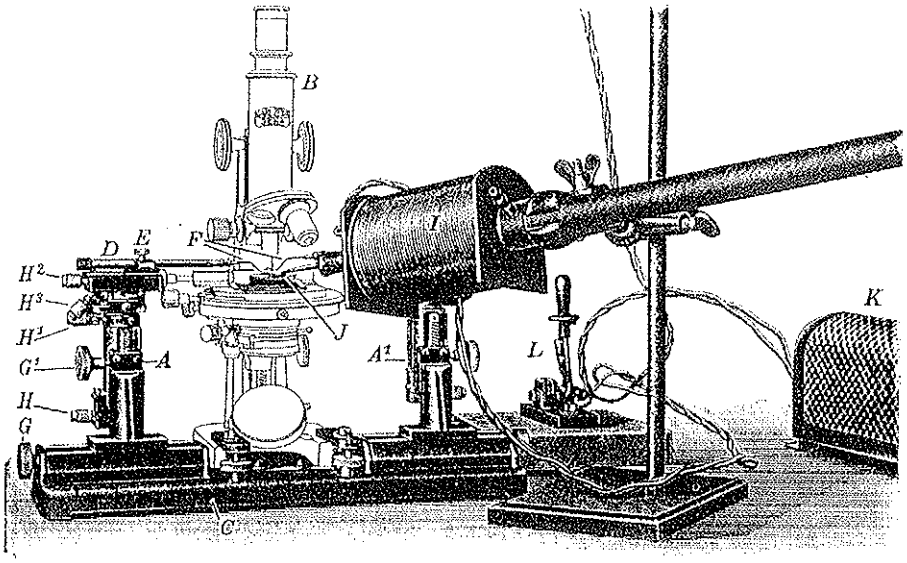

Fig. 2-10. A magnetic manipulation system to measure viscoelasticity in a single cell. From Freundlich and Seifriz, 1922.

to video rates for displacement detection when using the force method. Rotations can be detected by induction for ensembles of particles.

One of the first reports of an apparatus to measure intracellular viscoelasticity was from Freundlich and Seifriz (1922). A diagram of the instrument is shown in Fig. 2-10.

In this instrument, a micromanipulator mounted next to the microscope objective was used to insert a magnetic particle, made of nickel or magnetite, into a relatively large cell like a sand dollar egg. Then a magnetic field gradient, produced by an electromagnet placed as close as possible to the cell, was used to impose a force on the bead, whose displacement was measured by the microscope. The strength of the force on the bead could be calibrated by measuring the rate of its movement through a calibration fluid of viscosity that could be measured by conventional rheometers. This magnetic manipulation instrument was the precursor of current magnet-based microrheology systems, and was further enhanced by work of Crick and Hughes (1950), who made two important modifications of the experimental design. One was to first magnetize the particle with a large magnetic field, and then use a smaller probing magnetic field directed at a different angle to twist particles on or within the cell. The second change was to use phagocytic cells that would engulf the magnetic particle, thereby avoiding possible damage to the cell when magnetic particles were forced through its membrane. These early studies were done before the cytoskeleton was visualized by electron or fluorescence microscopy and before the phospholipid bilayer forming the cell membrane was characterized, so a critical evaluation could not be done of how disruptive either way of introducing the beads was. Further pioneering work was done on amoebae (Yagi, 1961) and on squid axoplasm (Sato et al., 1984).

In principle, the motion of embedded probes will depend on the probe size. Small particles can diffuse through the meshes, and this has been used to determine effective mesh sizes in model systems (Jones and Luby-Phelps, 1996; Schmidt et al., 1989; Schnurr et al., 1997) and in cells (Jones et al., 1997; Luby-Phelps, 1994; Valentine et al., 2001). On the other hand, the beads might interact with and stick to the cytoskeleton, possibly mediated by an enveloping lipid membrane and by motor proteins, which would cause active motion. How micron-sized beads are coupled to the network in which they are imbedded is still a major issue in evaluating microrheology measurements, and no optimal method to control or prevent interactions yet exists. Entry of a particle through phagocytosis certainly places it in a compartment distinct from the proteins forming the cytoskeleton, and how such phagosomes are bound to other cytoplasmic structures is unclear. Likewise, both the mechanical and chemical effects of placing micron-sized metal beads in the cell raises issues about alignment and reorganization of the cytoskeleton. These issues will be further considered in the following sections.

Pulling by magnetic field gradients

Magnetic particles can either be inserted into cells or bound – possibly via specific attachments – to cell surfaces. Both superparamagnetic particles (Bausch et al., 1998; Keller et al., 2001) and ferro- as well as ferrimagnetic particles (Bausch et al., 1999; Trepat et al., 2003; Valberg and Butler, 1987) have been used. Paramagnetic particles will experience a translational force in a field gradient, but no torque. With sharpened iron cores reaching close to the cells, forces of up to 10 nN have been generated (Vonna et al., 2003). Ferromagnetic (as well as ferrimagnetic) particles have larger magnetic moments and therefore need less-strong gradients, which can be produced by electromagnetic coils without iron cores and can therefore be much more rapidly modulated. The particles have to be magnetized initially with a strong homogeneous field. Depending on the directions of the fields, particles will experience both torque and translational forces in a field gradient (see Fig. 2-11). Forces reported are on the order of pN (Trepat et al., 2003).

Forces exerted by the cell in response to an imposed particle movement, both on the membrane and inside the cell, are mostly dominated by the cytoskeleton. Exceptions are cases where the particle size is smaller than the cytoskeletal mesh size; specialized cells, such as mammalian red blood cells without a three-dimensional cytoskeleton; or cells with a disrupted cytoskeleton after treatment with drugs such as nocodazole or cytochalasin. The interpretation of measured responses needs to start from a knowledge of the exact geometry of the surroundings of the probe and it is difficult, even when the particle is inserted deeply into the cell. This is due to the highly inhomogeneous character of the cytoplasm, consisting of different types of protein fibers, bundles, organelles, and membranes. Because a living cell is an active material that is slowly and continuously changing shape, responses are in general time dependent and contain passive and active components. Passive responses to low forces are often hidden under the active motions of the cell, while responses to large forces do not probe linear response parameters, but rather nonlinear behavior and rupture of the networks. Given all the restrictions mentioned, a window to measure

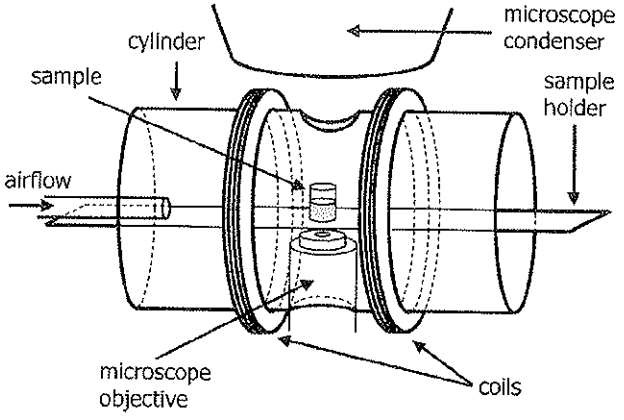

Fig. 2-11. Schematic diagram of a magnetic tweezers device using a magnetic field gradient. From Trepat et al., 2003.

the passive mechanical properties of cells appears to be to apply large strains, or to apply relatively high-frequency oscillatory strain at small amplitudes, while active responses can best be measured at low frequencies.

A number of experiments performed inside cells have observed the creep response to the instantaneous application of large or small forces (Bausch et al., 1999; Bausch et al., 1998; Feneberg et al., 2001). Bulk shear moduli were found to vary from ~20 Pa in the cytoplasm of Dictyostelium to ~300 Pa inside macrophages. At higher forces and strains, differences in rupture forces were found between mutant Dictyostelium cells and wild-type controls, highlighting the roles of regulatory proteins for the properties of the cytoskeleton (Feneberg et al., 2001).

With particles attached to the surface of cells, a shear modulus between 20 and 40 kPa was measured in the cortex of fibroblasts (Bausch et al., 1998), qualitative differences were measured between unstimulated and stimulated (stiffening) vascular endothelial cells (Bausch et al., 2001), and an absolute value of about 400 Pa was estimated from subsequent work (Feneberg et al., 2004). Active responses of macrophages and the formation of cell protrusion under varying forces were also tested with externally attached magnetic beads (Vonna et al., 2003).

Twisting of magnetized particles on the cell surface and interior

Applying a pure torque to magnetic particles avoids the difficulties of constructing a well-controlled field gradient. Homogeneous fields can be created rather easily. The method most widely used was pioneered by Valberg and colleagues (Valberg and Butler, 1987; Valberg and Feldman, 1987; Wang et al., 1993) and consists of using a strong magnetic field pulse to magnetize a large number of ferromagnetic particles that were previously attached to an ensemble (20,000–40,000) of cells. A weaker probe field oriented at 90° to the induced dipoles then causes rotation, which is measured in a lock-in mode with a magnetometer. In an homogeneous infinite medium, an effective shear modulus can be determined simply from the angle α rotated in response to an applied torque T: $G = T/\alpha$. On the surface of cells, however,

the boundary conditions are highly complex, and a substantial polydispersity within the bead ensemble is expected (Fabry et al., 1999). Therefore the method has been mainly used for determining qualitative behavior, for comparative studies of different cell types, and for studies of relative changes in a given cell population. Frequency dependence of the viscoelastic response was measured with smooth muscle cells between 0.05 and 0.4 Hz (Maksym et al., 2000) and with bronchial epithelial cells up to 16 Hz (Puig-de-Morales et al., 2001) (see also Chapter 3). The shear elastic modulus was found to be around 50 Pa with a weak frequency dependence in both cases.

Rotation in response to torque can also be detected on individual particles by video tracking when beads are attached to the outsides of cells. In that case the torque causes center-of-mass displacement, which can be tracked with nm accuracy (Fabry et al., 2001). Tracking individual particles makes it possible to study the heterogeneity of response between different cells and in different locations on cells. In conjunction with fluorescent labeling it is possible to explore the strains caused by locally imposed stresses; initial studies reveal that the strain field is surprisingly long-range (Hu et al., 2003). Using oscillatory torque and phase-locking techniques, the bandwidth of this technique was extended to 1 kHz (Fabry et al., 2001). While absolute shear moduli were still not easy to determine because of unknown geometrical factors such as depth of embedding, the bandwidth was wide enough to study the scaling behavior of the complex shear modulus more extensively. The observed weak power-laws (exponent between 0.1 and 0.3) appear to be rather typical for cells in that frequency window and were interpreted in terms of a soft glass model. Finite element numerical modeling has been applied to analyze the deformations of cells when attached magnetic beads are rotated (Mijailovich et al., 2002) to test the limits of linearity in the response as well as the effect of finite cell thickness and surface attachment.

Passive microrheology

To measure the viscoelastic properties of a system, it is not necessary to apply external forces when one employs microscopic probes. In a soft-enough medium, thermal fluctuations will be measurable and these fluctuations precisely report the linear-response viscoelastic parameters of the medium surrounding the probe. This connection is formalized in the fluctuation-dissipation (FD) theorem of linear-response theory (Landau et al., 1980). When possible, that is when the medium is soft enough, this method even elegantly circumvents the need to extrapolate to zero-force amplitude, which is usually necessary in active methods to obtain linear response parameters. Particularly in networks of semiflexible polymers such as the cytoskeleton, nonlinear response occurs typically for rather small strains on the order of a few percent (Storm et al., 2005).

A microscopic probe offers both the possibility to study inhomogeneities directly in the elastic properties of the cytoskeleton, and to measure viscoelasticity at higher frequencies, above 1 kHz or even up to MHz, because inertia of both probe and embedding medium can be neglected at such small length scales (Levine and Lubensky, 2001; Peterman et al., 2003b). The possibility to observe thermal fluctuations instead of actively applying force or torque in principle exists for all the techniques using

microscopic probes described above. It has, however, mainly been used in several related and recently developed techniques, collectively referred to as passive microrheology, employing beads of micron size embedded in the sample (Addas et al., 2004; Lau et al., 2003; MacKintosh and Schmidt, 1999; Mason et al., 1997; Schmidt et al., 2000; Schnurr et al., 1997). Passive microrheology has been used to probe, on microscopic scales, the material properties of systems ranging from simple polymer solutions to the interior of living cells.

Optically detected individual probes

The simplest method in terms of instrumentation uses video microscopy to record the Brownian motion of the embedded particles. Advantages are the use of standard equipment coupled with well-established image processing and particle tracking (Crocker and Grier, 1996), and the fact that massively parallel processing can be done (100 s of particles at the same time). Disadvantages are the relatively low spatial and temporal resolution, although limits can be pushed to nm in spatial displacement resolution and kHz temporal resolution with specialized cameras. Much higher spatial and temporal resolution still can be achieved using laser interferometry with laser beams focused on individual probe particles (Denk and Webb, 1990; Gittes and Schmidt, 1998; Pralle et al., 1999). Due to high light intensities focused on the particles, high spatial resolution (sub-nm) can be reached. Because the detection involves no video imaging, 100 kHz bandwidth can be reached routinely.

One-particle method

Once particle positions as a function of time are recorded by either method, the complex shear modulus $G(\omega)$ of the viscoelastic particle environment has to be calculated. This can be done by calculating the mean square displacement $\langle x_\omega^2 \rangle$ of the Brownian motion by Fourier transformation. The complex compliance $\alpha(\omega)$ of the probe particle with respect to a force exerted on it is defined by:

$$x_\omega = (\alpha' + i\alpha'') f_\omega \tag{2.12}$$

The FD theorem relates the imaginary part of the complex compliance to the mean square displacement:

$$\langle x_\omega^2 \rangle = \frac{4k_B T \alpha''}{\omega}. \tag{2.13}$$

Using a Kramers-Kronig relation (Landau et al., 1980):

$$\alpha'(\omega) = \frac{2}{\pi} P \int_0^\infty \frac{\zeta \alpha''(\zeta)}{\zeta^2 - \omega^2} d\zeta, \tag{2.14}$$

where ζ is the frequency variable to integrate over and P denotes a principal value integral, one can then calculate the real part of the compliance. Knowing both real and imaginary parts of the compliance, one then finds the complex shear modulus via

a generalized Stokes law:

$$\alpha(\omega) = \frac{1}{6\pi G(\omega) R}, \tag{2.15}$$

where R is the probe bead radius. This procedure is explained in detail in Schnurr et al. (1997).

The shear modulus can also be derived from position fluctuation data in a different way. After first calculating the mean square displacement as a function of time, one can obtain (using equipartition) a viscoelastic memory function by Laplace transformation, The shear modulus follows by again using the generalized Stokes law (Mason et al., 1997).

Two-particle methods

Large discrepancies between macroscopic viscoelastic parameters and those determined by one-particle microrheology can arise if the presence of the probe particle itself influences the viscoelastic medium in its vicinity or if active particle movement occurs and is interpreted as thermal motion. The shear strain field coupled to the motion of a probe particle extends into the medium a distance that is similar to the particle radius. Any perturbation of the medium caused by the presence of the particle will decay over a distance that is the shorter of the particle radius or characteristic length scales in the medium itself, such as mesh size of a network or persistence length of a polymer. Thus it follows that if any characteristic length scales in the system exceed the probe size, the simple interpretation of data with the generalized Stokes law is not valid. This is probably always the case when micron-sized beads are used to study the cytoskeleton, because the persistence length of actin is already 17 μm (Howard, 2001), while that of actin bundles or microtubules is much larger still. A perturbation of the medium could be caused by a chemical interaction with the probe surface, which can be prevented by appropriate surface coating. It is unavoidable, though, that the probe bead locally dilutes the medium by entropic depletion. To circumvent these pitfalls, two-particle microrheology has been developed (Crocker et al., 2000; Levine and Lubensky, 2000). In this variant, the cross-correlation of the displacement fluctuations of two particles, located at a given distance from each other, is measured (Fig. 2-12). The distance between the probes takes over as relevant length scale and probe size or shape become of secondary importance.

Instead of the one-particle compliance, a mutual compliance is defined by:

$$x_\omega^{mi} = \alpha_{ij}^{mn}(\omega) f_\omega^{nj}, \tag{2.16}$$

with particle indices n, m and coordinate indices i, $j = x$, y. If the particles are separated by a distance r along the x-axis, two cases are relevant, namely α_{xx}^{12}, which will be denoted as $\alpha_{\parallel}^{12}$, and α_{yy}^{12}, which will be denoted as $\alpha_{\perp}^{12}$ (the other combinations are second order). The Fourier transform of the cross-correlation function is related to the imaginary part of the corresponding compliance:

$$S_{ij}^{12}(\omega) = X_i^1(\omega) X_j^2(\omega)^\dagger = \frac{4k_B T}{\omega} \alpha_{ij}^{12''}(\omega), \tag{2.17}$$

where $\dagger$ denotes the complex conjugate.

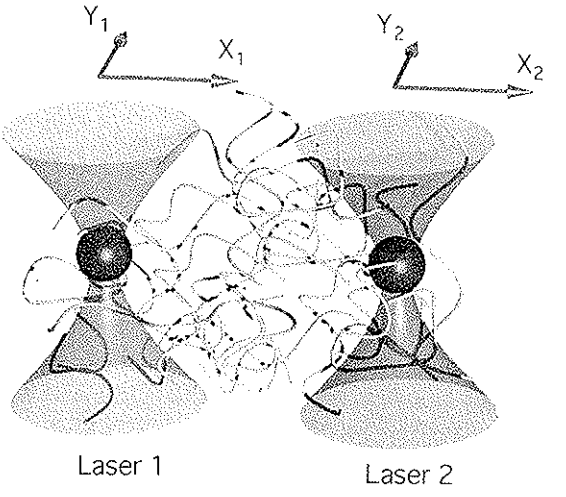

Fig. 2-12. Sketch of 1-particle and 2-particle microrheology using lasers for trapping and detection. Either one laser beam is focused on one particle at a time, or the two beams, displaced by some distance, are each focused on seperate particles. In both cases the motion of the particle in the two directions normal to the laser propagation direction is measured by projecting the laser light onto quadrant photodiodes downstream from the sample.

A Kramers-Kronig integral can again be used to calculate the real parts, and elastic moduli can be derived according to Levine and Lubensky (2002) from:

$$\alpha_{\parallel}^{12}(\omega) = \frac{1}{4\pi r \mu_0(\omega)} \tag{2.18}$$

$$\alpha_{\perp}^{12}(\omega) = \frac{1}{8\pi r \mu_0(\omega)} \left[\frac{\lambda_0(\omega) + 3\mu_0(\omega)}{\lambda_0(\omega) + 2\mu_0(\omega)} \right], \tag{2.19}$$

written here (following Levine and Lubensky (2002)) with the Lamé coefficients $\lambda_0(\omega)$ and $\mu_0(\omega)$, where $\mu_0(\omega) = G(\omega)$. One can thus measure directly the compressional modulus and the shear modulus in the sample.

The technique can again be implemented using video recording and particle tracking (Crocker et al., 2000) or laser interferometry. In cells, so far only a video-based variant has been used (Lau et al., 2003), exploring the low-frequency regime of the cellular dynamics in mouse macrophages and mouse carcinoma cells. It was found that the low-frequency passive microrheology results were strongly influenced by active transport in the cells, so that the fluctuation-dissipation theorem could not be used for calculating viscoelastic parameters.

Dynamic light scattering and diffusing wave spectroscopy

A well-established method to study the dynamics of large ensembles of particles in solutions is dynamic light scattering (DLS) (Berne and Pecora, 1990). To obtain smooth data and good statistics, it is obviously advantageous to average over a large number of particles. In DLS, a collimated laser beam is typically sent through a sample of milliliter volume, and scattered light is collected under a well-defined

angle with a photomultiplier or other sensitive detector. The intensity autocorrelation function:

$$g_2(\tau) = \frac{\langle I(t)I(t+\tau)\rangle}{\langle I(t)\rangle^2} = 1 + \beta e^{-q^2\langle \Delta r^2(\tau)\rangle/3} \tag{2.20}$$

can be used to calculate the average mean square displacement $\langle \Delta r^2(\tau)\rangle$ of particles, with the scattering vector $q = 4\pi n \sin(\theta/2)/\lambda$, wavelength λ, scattering angle θ and index of the solvent n, and a coherence factor β. This relationship assumes that all particles are identical and that the solution is homogeneous across the scattering volume. It also assumes that the particles dominate the scattering intensity compared to the scattering from the embedding medium itself. DLS has also been used extensively to study polymer solutions without added probe particles (Berne and Pecora, 1990). In that case the medium has to be modeled to extract material properties from the observed intensity autocorrelation function. This has been done for example for pure actin networks as models for the cytoskeleton of cells (Isambert et al., 1995; Liverpool and Maggs, 2001; Schmidt et al., 1989). Unfortunately this technique is not well applicable to study the interior of cells, because the cellular environment is highly inhomogeneous and it is not well defined which structures scatter the light in any given location. Larger objects dominate the scattered intensity (Berne and Pecora, 1990). DLS has been applied to red blood cells (Peetermans et al., 1987a; Peetermans et al., 1987b), but results have been qualitative. It is also difficult to introduce external probe particles that scatter light strongly enough in sufficient concentrations without harming the cells.

A related light-scattering technique is diffusing wave spectroscopy (DWS) (Pine et al., 1988; Weitz et al., 1993), which measures again intensity correlation functions of scattered light, but now in very dense opaque media where light is scattered many times before it is detected so that the path of a photon becomes a random walk and resembles diffusion. There is no more scattering-vector dependence in the field correlation function, which is directly related to the average mean square displacement $\langle \Delta r^2(\tau)\rangle$ of the scattering particles (Weitz and Pine, 1993):

$$g_1(\tau) \propto \int_0^\infty P(s) \exp\left[-\frac{k_0^2 s \langle \Delta r^2(\tau)\rangle}{3l^*}\right] ds. \tag{2.21}$$

$P(s)$ is the probability that the light travels a path length s, $k_0 = 2\pi/\lambda$ is the wave vector, and l^* is the transport mean free path. The final steps to extract a complex shear modulus are the same as described above, either using the power spectral density method (Schnurr et al., 1997) or the Laplace transform method (Mason et al., 1997).

The advantage of the technique is that it is sensitive to very small motions (of less than nm) because the path of an individual photon reflects the sum of the motions of the all particles by which it is scattered. The bandwidth of the technique is also high (typically 10 Hz to 1 MHz), so that ensemble-averaged mean-square displacements, and from that viscoelastic response functions, can be measured over many decades in frequency. The technique has been used to study polymer solutions, colloidal systems, and cytoskeletal protein solutions (actin) (Mason et al., 1997; Mason et al., 2000) and

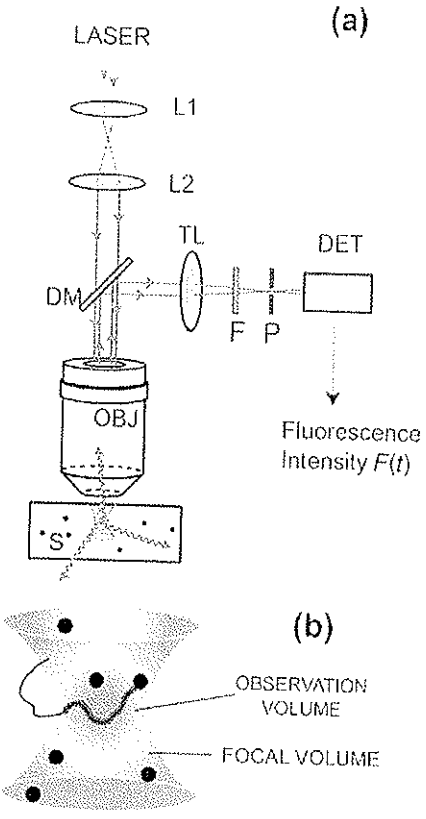

Fig. 2-13. (a) Experimental set-up for fluorescence correlation spectroscopy. A laser beam is expanded (L1, L2) and focussed through a microscope objective into a fluorescent sample. The fluorescence light is collected through the same objective and split out with a dichroic mirror toward the confocal pinhole (P) and then the detector. (b) Magnified focal volume with the fluorescent particles (spheres) and the diffusive path of one particle highlighted. From Hess et al., 2002.

results agree with those from conventional methods in the time/frequency regimes where they overlap. The application to cells is hindered, just as in the case of DLS, by the inhomogeneity of the cellular environment. Furthermore, typical cells are more or less transparent, in other words one would need to introduce high concentrations of scattering particles, which likely would disturb the cell's integrity.

Fluorescence correlation spectroscopy

Many complications can be avoided if specific particles or molecules of interest in a cell can be selected from other structures. A way to avoid collecting signals from unknown cellular structures is to use fluorescent labeling of particular molecules or structures within the cell. This method is extensively used in cell biology to study the localization of certain proteins in the cell. Fluorescence can also be used to measure dynamic processes in video microscopy, but due to low emission intensities of fluorescent molecules and due to their fast Brownian motion when they are not fixed to larger structures, it is difficult to use such data to extract diffusion coefficients or viscoelastic parameters inside cells. A method that is related to dynamic light scattering and is a nonimaging method that can reach much faster time scales is fluorescence correlation spectroscopy (Hess et al., 2002; Webb, 2001), where a laser is focused to a small volume and the fluctuating fluorescence originating from molecules entering and leaving this volume is recorded with fast detectors (Fig. 2-13).

From the fluorescence intensity fluctuations $\delta F(t) = F(t) - \langle F(t) \rangle$ one calculates the normalized autocorrelation function:

$$G(\tau) = \frac{\langle \delta F(t) \delta F(t+\tau) \rangle}{\langle F(t) \rangle^2}, \tag{2.22}$$

from which one can calculate in the simplest case, in the absence of chemical reactions involving the fluorescent species, the characteristic time τ_D a diffusing molecule spends in the focal volume:

$$G_D(\tau) = \frac{1}{N(1+\tau/\tau_D)(1+\tau/\omega^2\tau_D)^{1/2}} \tag{2.23}$$

with an axial-to-lateral-dimension ratio ω and the mean number of fluorescent molecules in the focus N. Eq. 2.23 is valid for a molecule diffusing in 3D. The method can also be used in other cases, for example 2D diffusion in a membrane.

With some knowledge of the geometry of the situation – for example 2D membrane-bound diffusion – one can again extract diffusion coefficients. This has been done on cell surfaces and even inside cells (see references in Hess et al., (2002)). Data typically have been interpreted as diffusion in a purely viscous environment or as diffusion in an inhomogeneous environment with obstacles. Compared with the rheology methods described above, fluorescence correlation spectroscopy is particularly good when studying small particles such as single-enzyme molecules. For the motion of such particles it is not appropriate to model the environment inside a cell as a viscoelastic continuum, because characteristic length scales of the cytoskeleton are as large or larger than the particles.

Optical stretcher

A novel optical method related to optical traps employs two opposing nonfocused laser beams to both immobilize and stretch a suspended cell (Guck et al., 2001; Guck et al., 2000). Viscoelastic properties are determined from the time-dependent change in cell dimensions as a function of optical pressures. This method has the significant advantage over other optical trapping methods that it can be scaled up and automated to allow measurement, and potentially sorting, of many cells within a complex mixture for use in diagnosing abnormal cells and sorting cells on the basis of their rigidity (Lincoln et al., 2004).

Acoustic microscopy

Ultrasound transmission and attenuation through cells and biological tissues can also provide measurements of viscoelasticity, and acoustic microscopy has the potential to provide high-resolution imaging of live cells in a minimally invasive manner (Viola and Walker, 2003). Studies of purified systems such as F-actin (Wagner et al., 2001; Wagner et al., 1999), and alginate capsules (Klemenz et al., 2003), suggest that acoustic signals can be related to changes in material properties of these biopolymer gels, but there are numerous challenges related to interpreting the data and relating them

to viscoelastic parameters before the potential of this method for quantitative high-resolution elastic imaging on cells is realized.

Outstanding issues and future directions

The survey of methods used to study the rheology of cells presented here shows the wide range of methods that various groups have designed and employed. At present there appears to be no one ideal method suitable for most cell types. In many cases, measurements of similar cell types by different methods have yielded highly different values for elastic and viscous parameters. For example, micropipette aspiration of leukocytes can variably be interpreted as showing that these cells are liquid droplets with a cortical tension or soft viscoelastic fluids, while atomic force microscopy measures elastic moduli on the order of 1000 Pa. In part, differences in measurements stem from differences in the time scale or frequency and in the strains at which the measurements are done. Also, it is almost certain that cells respond actively to the forces needed to measure their rheology, and the material properties of the cell often cannot be interpreted as those of passive material. Combining rheological measurements with simultaneous monitoring or manipulation of intracellular signals and cytoskeletal structures can go a long way toward resolving such challenges.

Currently a different and equally serious challenge is presented by the finding that even when studying purified systems like F-actin networks, micro- and macrorheology methods sometimes give very different results, for reasons that are not completely clear. In part there are likely to be methodological problems that need to be resolved, but it also appears that there are interesting physical differences in probing very small displacements of parts of a network not much larger than the network mesh size and the macroscopic deformations that occur as the whole network deforms in macrorheologic measurements. Here a combination of more experimentation and new theories is likely to be important.

The physical properties of cells have been of great interest to biologists and physiologists from the earliest studies that suggested that cells may be able to convert from solid to liquid states as they move or perform other functions. More recently, unraveling the immense complexity of the molecular biology regulating cell biology and high-resolution imaging of intracellular structures have provided molecular models to suggest how the dynamic viscoelasticity of the cell may be achieved. Now the renewed interest in cell mechanics together with technological advances allowing unprecedented precision and sensitivity in force application and imaging can combine with molecular information to increase our understanding of the mechanisms by which cells maintain and change their mechanical properties.

References

Addas KM, Schmidt CF, Tang JX. (2004). "Microrheology of solutions of semiflexible biopolymer filaments using laser tweezers interferometry." *Phys. Rev. E.*, **70**(2):Art. No. 021503.

Agayan RR, Gittes F, Kopelman R, Schmidt CF. (2002). "Optical trapping near resonance absorption." *Appl. Opt.*, **41**(12):2318–27.

Ashkin A. (1992). "Forces of a single-beam gradient laser trap on a dielectric sphere in the ray optics regime." *Biophys. J.*, **61**(2):569–82.

Ashkin A. (1997). "Optical trapping and manipulation of neutral particles using lasers." *Proc. Natl. Acad. Sci. USA*, **94**(10):4853–60.

Ashkin A, Dziedzic JM, Bjorkholm JE, Chu S. (1986). "Observation of a single-beam gradient force optical trap for dielectric particles." *Opt. Lett.*, **11**(5):288–90.

Bacabac RG, Smit TH, Heethaar RM, van Loon JJWA, Pourquie MJMB, Nieuwstadt FTM, Klein-Nulend J. (2002). "Characteristics of the parallel-plate flow chamber for mechanical stimulation of bone cells under microgravity." *J. Gravitat. Physiol.*, **9**:P181–2.

Bacabac RG, Smit TH, Mullender MG, Dijcks SJ, Van Loon J, Klein-Nulend J. (2004). "Nitric oxide production by bone cells is fluid shear stress rate dependent." *Biochem. Biophys. Res. Commun.*, **315**(4):823–9.

Barbee KA, Mundel T, Lal R, Davies PF. (1995). "Subcellular distribution of shear stress at the surface of flow-aligned and nonaligned endothelial monolayers." *Am. J. Physiol.*, **268**(4 Pt 2): H1765–72.

Bausch AR, Hellerer U, Essler M, Aepfelbacher M, Sackmann E. (2001). "Rapid stiffening of integrin receptor-actin linkages in endothelial cells stimulated with thrombin: A magnetic bead microrheology study." *Biophys. J.*, **80**(6):2649–57.

Bausch AR, Moller W, Sackmann E. (1999). "Measurement of local viscoelasticity and forces in living cells by magnetic tweezers." *Biophys. J.*, **76**(1):573–9.

Bausch AR, Ziemann F, Boulbitch AA, Jacobson K, Sackmann E. (1998). "Local measurements of viscoelastic parameters of adherent cell surfaces by magnetic bead microrheometry." *Biophys. J.*, **75**(4):2038–49.

Berne BJ, Pecora R. 1990. *Dynamic light scattering*. Malabar: Robert E. Krieger Publishing Co.

Binnig G, Quate CF, Gerber C. (1986). "Atomic Force Microscope." *Phys., Rev., Lett.*, **56**(9):930–3.

Bray D. (1984). "Axonal growth in response to experimentally applied mechanical tension." *Dev. Biol.*, **102**(2):379–89.

Burger EH, Klein-Nulend J. (1999). "Mechanotransduction in bone – role of the lacuno-canalicular network." *Faseb. J.*, **13**:S101–S112.

Caille N, Thoumine O, Tardy Y, Meister JJ. (2002). "Contribution of the nucleus to the mechanical properties of endothelial cells." *J. Biomech.*, **35**(2):177–87.

Charras GT, Horton MA. (2002). "Determination of cellular strains by combined atomic force microscopy and finite element modeling." *Biophys. J.*, **83**(2):858–79.

Chien S, Schmid-Schonbein GW, Sung KL, Schmalzer EA, Skalak R. (1984). "Viscoelastic properties of leukocytes." *Kroc. Found Ser.*, **16**:19–51.

Crick F, Hughes A. (1950). "The physical properties of cytoplasm." *Exp. Cell Res.*, 1:37–80.

Crocker JC, Grier DG. (1996). "Methods of digital video microscopy for colloidal studies." *J. Colloid. Interface Sci.*, **179**(1):298–310.

Crocker JC, Valentine MT, Weeks ER, Gisler T, Kaplan PD, Yodh AG, Weitz DA. (2000). "Two-point microrheology of inhomogeneous soft materials." *Phys. Rev. Lett.*, **85**(4):888–91.

Cunningham CC, Gorlin JB, Kwiatkowski DJ, Hartwig JH, Janmey PA, Byers HR, Stossel TP. (1992). "Actin-binding protein requirement for cortical stability and efficient locomotion." *Science*, **255**(5042):325–7.

Daily B, Elson EL, Zahalak GI. (1984). "Cell poking. Determination of the elastic area compressibility modulus of the erythrocyte membrane." *Biophys. J.*, **45**(4):671–82.

Dao M, Lim CT, Suresh S. (2003). "Mechanics of the human red blood cell deformed by optical tweezers." *J. Mechan. Phys. Solids*, **51**(11–12):2259–80.

Davies PF, Remuzzi A, Gordon EJ, Dewey CF, Jr., Gimbrone MA, Jr. (1986). "Turbulent fluid shear stress induces vascular endothelial cell turnover in vitro." *Proc. Natl. Acad. Sci. USA*, **83**(7): 2114–17.

de Pablo PJ, Colchero J, Gomez-Herrero J, Baro AM. (1998). "Jumping mode scanning force microscopy." *Appl. Phys. Lett.*, **73**(22):3300–2.

Denk W, Webb WW. (1990). "Optical measurement of picometer displacements of transparent microscopic objects." *Appl. Opt.*, **29**(16):2382–91.

Desprat N, Richert A, Simeon J, Asnacios A. (2005). "Creep function of a single living cell." *Biophys. J.*, **88**(3):2224–33.

Dewey CF, Jr., Bussolari SR, Gimbrone MA, Jr., Davies PF. (1981). "The dynamic response of vascular endothelial cells to fluid shear stress." *J. Biomech. Eng.*, **103**(3):177–85.

Discher DE, Mohandas N, Evans EA. (1994). "Molecular maps of red cell deformation: hidden elasticity and in situ connectivity." *Science*, **266**(5187):1032–5.

Dong C, Skalak R, Sung KL, Schmid SG, Chien S. (1988). "Passive deformation analysis of human leukocytes." *J. Biomech. Eng.*, **110**(1):27–36.

Dufrene YF. (2003). "Recent progress in the application of atomic force microscopy imaging and force spectroscopy to microbiology." *Curr. Op. Microbiol.*, **6**(3):317–23.

Dvorak JA, Nagao E. (1998). "Kinetic analysis of the mitotic cycle of living vertebrate cells by atomic force microscopy" *Exp. Cell Res.*, **242**:69–74.

Ehrlich PJ, Lanyon LE. (2002). "Mechanical strain and bone cell function: a review." *Osteoporos. Int.*, **13**(9):688–700.

Eichinger L, Koppel B, Noegel AA, Schleicher M, Schliwa M, Weijer K, Witke W, Janmey PA. (1996). "Mechanical perturbation elicits a phenotypic difference between Dictyostelium wild-type cells and cytoskeletal mutants." *Biophys. J.*, **70**(2):1054–60.

Evans E, Yeung A. (1989). "Apparent viscosity and cortical tension of blood granulocytes determined by micropipet aspiration." *Biophys. J.*, **56**(1):151–60.

Evans EA, Hochmuth RM. (1976). "Membrane viscoelasticity." *Biophys. J.*, **16**(1):1–11.

Fabry B, Maksym GN, Butler JP, Glogauer M, Navajas D, Fredberg JJ. (2001). "Scaling the microrheology of living cells." *Phys. Rev. Lett.*, **8714**(14):Art. No.148102.

Fabry B, Maksym GN, Hubmayr RD, Butler JP, Fredberg JJ. (1999). "Implications of heterogeneous bead behavior on cell mechanical properties measured with magnetic twisting cytometry." *J. Magn. and Magn. Mater.*, **194**(1–3):120–5.

Feneberg W, Aepfelbacher M, Sackmann E. (2004). "Microviscoelasticity of the apical cell surface of human umbilical vein endothelial cells (HUVEC) within confluent monolayers." *Biophys. J.*, **87**(2):1338–50.

Feneberg W, Westphal M, Sackmann E. (2001). "Dictyostelium cells' cytoplasm as an active viscoplastic body." *Eur. Biophys. J.*, **30**(4):284–94.

Florian JA, Kosky JR, Ainslie K, Pang ZY, Dull RO, Tarbell JM. (2003). "Heparan sulfate proteoglycan is a mechanosensor on endothelial cells." *Circul. Res.*, **93**(10):E136–42.

Freundlich H, Seifriz W. (1922). "Über die Elastizität von Sollen und Gelen." *Z. Phys. Chem.*, **104**:233–61.

Fukuda S, Schmid-Schonbein GW. (2003). "Regulation of CD18 expression on neutrophils in response to fluid shear stress." *Proc. Natl. Acad. Sci. USA*, **100**(23):13152–7.

Gittes F, Schmidt CF. (1998). "Interference model for back-focal-plane displacement detection in optical tweezers." *Opt. Lett.*, **23**(1):7–9.

Glogauer M, Arora P, Yao G, Sokholov I, Ferrier J, McCulloch CA. (1997). "Calcium ions and tyrosine phosphorylation interact coordinately with actin to regulate cytoprotective responses to stretching." *J. Cell Sci.*, **110** (Pt 1):11–21.

Grodzinsky AJ, Levenston ME, Jin M, Frank EH. (2000). "Cartilage tissue remodeling in response to mechanical forces." *Annu. Rev. Biomed. Eng.*, **2**:691–713.

Guck J, Ananthakrishnan R, Mahmood H, Moon TJ, Cunningham CC, Kas J. (2001). "The optical stretcher: a novel laser tool to micromanipulate cells." *Biophys. J.*, **81**(2):767–84.

Guck J, Ananthakrishnan R, Moon TJ, Cunningham CC, Kas J. (2000). "Optical deformability of soft biological dielectrics." *Phys. Rev. Lett.*, **84**(23):5451–4.

Hansma PK, Cleveland JP, Radmacher M, Walters DA, Hillner PE, Bezanilla M, Fritz M, Vie D, Hansma HG, Prater CBet al. (1994). "Tapping Mode Atomic-Force Microscopy in Liquids." *Appl. Phys. Lett.*, **64**(13):1738–40.

Harada Y, Asakura T. (1996). "Radiation forces on a dielectric sphere in the Rayleigh scattering regime." *Opt. Commun.*, **124**(5–6):529–41.

Heidemann SR, Buxbaum RE. (1994). "Mechanical tension as a regulator of axonal development." *Neurotoxicology*, **15**(1):95–107.

Heidemann SR, Kaech S, Buxbaum RE, Matus A. (1999). "Direct observations of the mechanical behaviors of the cytoskeleton in living fibroblasts." *J. Cell Biol.*, **145**(1):109–22.

Heilbronn A. (1922). "Eine Neue Methode zur Bestimmung der Viskosität lebender Protoplasten" *Jahrb. Wiss. Botan*, **61**:284–338.

Heilbrunn L. 1952. *An outline of general physiology*. Philadelphia: WB Saunders. 818 p.

Heilbrunn L. 1956. *The dynamics of living protoplasm*. New York: Academic Press. 327 p.

Helmke BP, Rosen AB, Davies PF. (2003). "Mapping mechanical strain of an endogenous cytoskeletal network in living endothelial cells." *Biophys. J.*, **84**(4):2691–9.

Helmke BP, Thakker DB, Goldman RD, Davies PF. (2001). "Spatiotemporal analysis of flow-induced intermediate filament displacement in living endothelial cells." *Biophys. J.*, **80**(1):184–94.

Henon S, Lenormand G, Richert A, Gallet F. (1999). "A new determination of the shear modulus of the human erythrocyte membrane using optical tweezers." *Biophys. J.*, **76**(2):1145–51.

Hertz H. (1882). "Ueber den Kontakt elastischer Koerper." *J. Reine. Angew. Mathematik.* **92**:156–71.

Hess ST, Huang SH, Heikal AA, Webb WW. (2002). "Biological and chemical applications of fluorescence correlation spectroscopy: A review." *Biochem.*, **41**(3):697–705.

Hochmuth RM. (2000). "Micropipette aspiration of living cells." *J. Biomech.*, **33**(1):15–22.

Howard J. 2001. *Mechanics of motor proteins and the cytoskeleton*. Sunderland: Sinauer Associates.

Hu SH, Chen JX, Fabry B, Numaguchi Y, Gouldstone A, Ingber DE, Fredberg JJ, Butler JP, Wang N. (2003). "Intracellular stress tomography reveals stress focusing and structural anisotropy in cytoskeleton of living cells." *A. J. Physiol. -Cell Physiol.*, **285**(5):C1082–90.

Isambert H, Venier P, Maggs AC, Fattoum A, Kassab R, Pantaloni D, Carlier MF. (1995). "Flexibility of actin filaments derived from thermal fluctuations. Effect of bound nucleotide, phalloidin, and muscle regulatory proteins." *J. Biol. Chem.*, **270**(19):11437–44.

Jackson JD. 1975. *Class electrodyn*. New York: Wiley.

Janmey PA, Weitz DA. (2004). "Dealing with mechanics: mechanisms of force transduction in cells." *Trends Biochem. Sci.*, **29**(7):364–70.

Jones JD, LubyPhelps K. (1996). "Tracer diffusion through F-actin: Effect of filament length and cross-linking." *Biophys. J.*, **71**(5):2742–50.

Jones JD, Ragsdale GK, Rozelle A, Yin HL, Luby-Phelps K. (1997). "Diffusion of vesicle-sized particles in living cells is restricted by intermediate filaments." *Mol. Biol. Cell*, **8**:1006.

Keller M, Schilling J, Sackmann E. (2001). "Oscillatory magnetic bead rheometer for complex fluid microrheometry" *Rev. Sci. Instr.*, **72**(9):3626–34.

Kellermayer MS, Smith SB, Granzier HL, Bustamante C. (1997). "Folding-unfolding transitions in single titin molecules characterized with laser tweezers." *Science*, **276**(5315):1112–16.

Klein-Nulend J, Bacabac RG, Veldhuijzen JP, Van Loon JJWA. (2003). "Microgravity and bone cell mechanosensitivity" *Adv. Space Res.*, 32:1551–9.

Klemenz A, Schwinger C, Brandt J, Kressler J. (2003). "Investigation of elasto-mechanical properties of alginate microcapsules by scanning acoustic microscopy." *J. Biomed. Mater. Res.*, **65A**(2): 237–43.

Landau LD, Lifshitz EM. 1970. *Theory of elasticity*. New York: Pergamon Press.

Landau LD, Lifshitz EM, Pitaevskii LP. 1980. *Statist. phys*. Oxford, New York: Pergamon Press.

Lau AWC, Hoffman BD, Davies A, Crocker JC, Lubensky TC. (2003). "Microrheology, Stress Fluctuations and Active Behavior of Living Cells." *Phys. Rev. Lett.*, **91**:198101.

Lenormand G, Henon S, Richert A, Simeon J, Gallet F. (2001). "Direct measurement of the area expansion and shear moduli of the human red blood cell membrane skeleton." *Biophys. J.*, **81**(1): 43–56.

Levine AJ, Lubensky TC. (2000). "One- and two-particle microrheology." *Phys. Rev. Lett.*, **85**(8):1774–7.

Levine AJ, Lubensky TC. (2001). "The Response Function of a Sphere in a Viscoelastic Two-Fluid Medium." *Phys. Rev. E.*, **63**:0415101–12.

Levine AJ, Lubensky TC. (2002). "Two-point microrheology and the electrostatic analogy." *Phys. Rev. E. Stat. Nonlin. Soft. Matter. Phys.*, **65**:011501.

Lim CT, Dao M, Suresh S, Sow CH, Chew KT. (2004). "Large deformation of living cells using laser traps." *Acta. Mater.*, **52**(7):1837–45.

Lincoln B, Erickson HM, Schinkinger S, Wottawah F, Mitchell D, Ulvick S, Bilby C, Guck J. (2004). "Deformability-based flow cytometry." *Cytometry*, **59A**(2):203–9.

Liverpool TB, Maggs AC. (2001). "Dynamic scattering from semiflexible polymers." *Macromol*, **34**(17):6064–73.

Luby-Phelps K. (1994). "Physical-Properties of Cytoplasm." *Curr. Opin. Cell Biol.*, **6**(1):3–9.

MacKintosh FC, Schmidt CF. (1999). "Microrheology." *Curr. Opin. Colloid. & Inter. Sci.*, **4**(4): 300–7.

Mahaffy RE, Park S, Gerde E, Kas J, Shih CK. (2004). "Quantitative analysis of the viscoelastic properties of thin regions of fibroblasts using atomic force microscopy." *Biophys. J.*, **86**(3): 1777–93.

Mahaffy RE, Shih CK, MacKintosh FC, Kas J. (2000). "Scanning probe-based frequency-dependent microrheology of polymer gels and biological cells." *Phys. Rev. Lett.*, **85**(4):880–3.

Maksym GN, Fabry B, Butler JP, Navajas D, Tschumperlin DJ, Laporte JD, Fredberg JJ. (2000). "Mechanical properties of cultured human airway smooth muscle cells from 0.05 to 0.4 Hz." *J. Appl. Phys.*, **89**(4):1619–32.

Mason TG, Gang H, Weitz DA. (1997). "Diffusing-wave-spectroscopy measurements of viscoelasticity of complex fluids." *J. Opt. Soc. Am. A. Opt. & Image Sci.*, **14**(1):139–49.

Mason TG, Gisler T, Kroy K, Frey E, Weitz DA. (2000). "Rheology of F-actin solutions determined from thermally driven tracer motion." *J. Rheol.*, **44**(4):917–28.

Mijailovich SM, Kojic M, Zivkovic M, Fabry B, Fredberg JJ. (2002). "A finite element model of cell deformation during magnetic bead twisting." *J. Appl. Phys.*, **93**(4):1429–36.

Mitchison J, Swann M. (1954). "The mechanical properties of the cell surface. I: The cell elastimeter." *J. Exp. Biol.*, **31**:445–59.

Ohura N, Yamamoto K, Ichioka S, Sokabe T, Nakatsuka H, Baba A, Shibata M, Nakatsuka T, Harii K, Wada, et al. (2003). "Global analysis of shear stress-responsive genes in vascular endothelial cells." *J. Atheroscler. Thromb.*, **10**(5):304–13.

Peetermans JA, Matthews EK, Nishio I, Tanaka T. (1987a). "Particle Motion in Single Acinar-Cells Observed by Microscope Laser-Light Scattering Spectroscopy." *Eur. Biophys. J.*, **15**(2): 65–9.

Peetermans JA, Nishio I, Ohnishi ST, Tanaka T. (1987b). "Single Cell Laser-Light Scattering Spectroscopy in a Flow Cell – Repeated Sickling of Sickle Red-Blood-Cells." *Biochim. Biophys. Acta.*, **931**(3):320–5.

Peterman EJ, Gittes F, Schmidt CF. (2003a). "Laser-induced heating in optical traps." *Biophys. J.*, **84**(2 Pt 1):1308–16.

Peterman EJG, Dijk MAv, Kapitein LC, Schmidt CF. (2003b). "Extending the Bandwidth of Optical-Tweezers Interferometry." *Rev. Sci. Instrum.*, **74**(7):3246–9.

Petersen NO, McConnaughey WB, Elson EL. (1982). "Dependence of locally measured cellular deformability on position on the cell, temperature, and cytochalasin B." *Proc. Natl. Acad. Sci. USA*, **79**(17):5327–31.

Pine DJ, Weitz DA, Chaikin PM, Herbolzheimer E. (1988). "Diffusing Wave Spectroscopy." *Phys. Rev. Lett.*, **60**:1134.

Pralle A, Prummer M, Florin EL, Stelzer EHK, Horber JKH. (1999). "Three-dimensional high-resolution particle tracking for optical tweezers by forward scattered light." *Micros. Res. Tech.*, **44**(5):378–86.

Puig-de-Morales M, Grabulosa M, Alcaraz J, Mullol J, Maksym GN, Fredberg JJ, Navajas D. (2001). "Measurement of cell microrheology by magnetic twisting cytometry with frequency domain demodulation." *J. Appl. Phys.*, **91**(3):1152–59.

Putman CAJ, Vanderwerf KO, Degrooth BG, Vanhulst NF, Greve J. (1994). "Viscoelasticity of Living Cells Allows High-Resolution Imaging by Tapping Mode Atomic-Force Microscopy." *Biophys. J.*, **67**(4):1749–53.

Reiser P. (1949). "The protoplasmic viscosity of muscle." *Protoplasma*, **39**:95–8.

Richelme F, Benoliel AM, Bongrand P. (2000). "Dynamic study of cell mechanical and structural responses to rapid changes of calcium level." *Cell Motil. Cytoskel.*, **45**(2):93–105.

Rockwell MA, Fechheimer M, Taylor DL. (1984). "A comparison of methods used to characterize gelation of actin in vitro." *Cell Motil.*, **4**(3):197–213.

Rubin CT, Lanyon LE. (1984). "Regulation of Bone-Formation by Applied Dynamic Loads." *J. Bone. Joint Surgery-Am. Vol.*, **66A**(3):397–402.

Sato M, Wong TZ, Brown DT, Allen RD. (1984). "Rheological properties of living cytoplasm: A preliminary investigation of squid axoplasm (Loligo pealei)." *Cell Motil.*, **4**(1):7–23.

Schmidt CF, Barmann M, Isenberg G, Sackmann E. (1989). "Chain Dynamics, Mesh Size, and Diffusive Transport in Networks of Polymerized Actin – A Quasielastic Light Scattering and Microfluorescence Study." *Macromolecules.*, **22**(9):3638–49.

Schmidt FG, Hinner B, Sackmann E, Tang JX. (2000). "Viscoelastic Properties of Semiflexible Filamentous Bacteriophage fd." *Phys. Rev. E.*, **62**(4):5509–17.

Schnurr B, Gittes F, MacKintosh FC, Schmidt CF. (1997). "Determining microscopic viscoelasticity in flexible and semiflexible polymer networks from thermal fluctuations." *Macromol.*, **30**:7781–92.

Sleep J, Wilson D, Simmons R, Gratzer W. (1999). "Elasticity of the red cell membrane and its relation to hemolytic disorders: An optical tweezers study." *Biophys. J.*, **77**(6):3085–95.

Storm C, Pastore JJ, MacKintosh FC, Lubensky TC, Janmey PA. (2005). "Nonlinear Elasticity in Biological Gels." *Nature*:in press.

Stossel T. (1990). "How Cells Crawl." *Am. Scientist*, **78**:408–23.

Svoboda K, Block SM. (1994). "Biological applications of optical forces." *Annu. Rev. Biophys. Biomol. Struct.*, **23**:247–85.

Thoumine O, Ott A. (1997). "Time scale dependent viscoelastic and contractile regimes in fibroblasts probed by microplate manipulation." *J. Cell Sci.*, **110** (Pt 17):2109–16.

Thoumine O, Ott A, Cardoso O, Meister JJ. (1999). "Microplates: A new tool for manipulation and mechanical perturbation of individual cells." *J. Biochem. Biophys. Methods*, **39**(1–2): 47–62.

Trepat X, Grabulosa M, Buscemi L, Rico F, Fabry B, Fredberg JJ, Farre R. (2003). "Oscillatory magnetic tweezers based on ferromagnetic beads and simple coaxial coils." *Rev. Sci. Instr.*, **74**(9):4012–20.

Turner CH, Owan I, Takano Y. (1995). "Mechanotransduction in Bone – Role of Strain-Rate." *Am. J. Physiology-Endocrinol and Metab*, **32**(3):E438–42.

Valberg PA, Butler JP. (1987). "Magnetic Particle Motions within Living Cells – Physical Theory and Techniques." *Biophys. J.*, **52**(4):537–50.

Valberg PA, Feldman HA. (1987). "Magnetic Particle Motions within Living Cells – Measurement of Cytoplasmic Viscosity and Motile Activity." *Biophys. J.*, **52**(4):551–61.

Valentine MT, Kaplan PD, Thota D, Crocker JC, Gisler T, Prud'homme RK, Beck M, Weitz DA. (2001). "Investigating the microenvironments of inhomogeneous soft materials with multiple particle tracking." *Phys. Rev. E.*, **6406**(6):Art. No. 061506.

Viola F, Walker WF. (2003). "Radiation force imaging of viscoelastic properties with reduced artifacts." *IEEE Trans. Ultrason. Ferroelectr. Freq. Control*, **50**(6):736–42.

Vonna L, Wiedemann A, Aepfelbacher M, Sackmann E. (2003). "Local force induced conical protrusions of phagocytic cells." *J. Cell Sci.*, **116**(5):785–90.

Wagner O, Schuler H, Hofmann P, Langer D, Dancker P, Bereiter-Hahn J. (2001). "Sound attenuation of polymerizing actin reflects supramolecular structures: Viscoelastic properties of actin gels modified by cytochalasin D, profilin and alpha-actinin." *Biochem. J.*, **355**(Pt 3):771–8.

Wagner O, Zinke J, Dancker P, Grill W, Bereiter-Hahn J. (1999). "Viscoelastic properties of F-actin, microtubules, F-actin/alpha-actinin, and F-actin/hexokinase determined in microliter volumes with a novel nondestructive method." *Biophys. J.*, **76**(5):2784–96.

Wang N, Butler JP, Ingber DE. (1993). "Mechanotransduction across the Cell-Surface and through the Cytoskeleton." *Science*, **260**(5111):1124–27.

Waters CM, Sporn PH, Liu M, Fredberg JJ. (2002). "Cellular biomechanics in the lung." *Am. J. Physiol. Lung. Cell Mol. Physiol.*, **283**(3):L503–9.

Webb WW. (2001). "Fluorescence correlation spectroscopy: Inception, biophysical experimentations, and prospectus." *Appl. Opt.*, **40**(24):3969–83.

Weinbaum S, Zhang XB, Han YF, Vink H, Cowin SC. (2003). "Mechanotransduction and flow across the endothelial glycocalyx." *Proc. Natl. Acad. Sci. USA*, **100**(13):7988–95.

Weitz DA, Pine DJ. (1993). Diffusing-wave spectroscopy. In: Brown W, editor. *Dynamic light scattering*. Oxford: Oxford University Press.

Weitz DA, Zhu JX, Durian DJ, Gang H, Pine DJ. (1993). "Diffusing-Wave Spectroscopy – the Technique and Some Applications." *Physica. Scripta*, **T49B**:610–21.

Wolff J. 1986. *The law of bone remodelling*. Berlin: Springer.

Yagi K. (1961). "Mechanical and Colloidal Properties of Amoeba Protoplasm and Their Relations to Mechanism of Amoeboid Movement." *Comp. Biochem. Physiol.*, **3**(2):73–&.